Jpn. J. Appl. Phys. Vol. 42 (2003) pp. 7452–7455
Part 1, No. 12, December 2003

Dielectric Anomaly in Ferroelectric Liquid Crystals with Polarization Inversion

Chang-Jae YU, Sin-Doo LEE, Jung-Il JIN[1] and Jae-Hoon KIM[2*]

School of Electrical Engineering #32, Seoul National University, Kwanak P.O. Box 34, Seoul 151-742, Korea
[1]*Department of Chemistry, Korea University, Seoul 136-701, Korea*
[2]*Department of Physics, Hallym University, Chunchon, Kangwon-Do 200-702, Korea*

(Received May 6, 2003; accepted July 8, 2003; published December 10, 2003)

The dielectric anomaly in ferroelectric liquid crystals exhibiting polarization sign inversion has been studied as a function of temperature under an applied electric field. In such a system, the dielectric anomaly was introduced into a model of a dynamically fluctuating mixture of two interconvertible conformers, whose relative densities depended on temperature and external field. In the frame of the model, it was explained that dielectric constant increased after the suppression of the Goldstone mode by applying an electric field over a certain critical field. It was also found that the induced effective dipole moment, deduced from the field dependence of the dielectric constant, can be described by the simple power law as a function of temperature. [DOI: 10.1143/JJAP.42.7452]

KEYWORDS: ferroelectric liquid crystal, dielectric constant, anomaly

1. Introduction

Since the discovery of ferroelectricity in tilted chiral smectic phase,[1)] ferroelectric liquid crystals (FLCs) have been studied extensively for scientific understanding as well as for their device application. In most FLCs, spontaneous polarization, P_s, usually decreases with increasing temperature and vanishes at a smectic A-smectic C* (Sm A–Sm C*) phase transition temperature, which is described by the power law $P_s(T) = P_0(T_c - T)^{\alpha}$ where P_0, T_c, and α are a certain constant, the Sm A–Sm C* phase transition temperature, and a critical exponent, respectively.[2)]

The dielectric response of FLCs in a low-frequency regime consists of two modes connected to the relaxations of tilt and phase fluctuations of the director. These modes are commonly denoted the soft mode and the Goldstone mode, respectively.[3)] Although the soft mode greatly affects the dielectric properties of FLCs through Sm A–Sm C* phase transition, it is negligible with respect to the Goldstone mode in the Sm C* phase. Due to the contribution of the Goldstone mode corresponding to the collective director reorientations around a smectic cone, the dielectric constant of FLCs increases through Sm A–Sm C* phase transition and have a broad maximum at a few degrees below T_c.[3)] Applying an electric field in the Sm C* phase, the Goldstone mode is suppressed and reaches a certain constant value over a critical electric field.

However, depending on a subtle change in chemical structure,[4)] some chiral compounds have shown anomalous behavior in their dielectric constant with polarization inversion in the Sm C* phase.[5–11)] In such compounds, the dielectric constant has a local broad minimum value at a temperature T_i ($< T_c$), at which spontaneous polarization vanishes, in the case of a low dc bias field. Moreover, it slowly increases after the suppression of the Goldstone mode by applying an electric field over a certain critical field.

In this work, to describe this anomalous dielectric behavior with polarization inversion, we introduce the effective dipole moment obtained from the field dependence of dielectric constant into a model based on a dynamically fluctuating mixture of at least two interconvertible via an activation energy with changing temperature and external field.

2. Experimental

The chiral compounds used in this work were *s*-2-methylbuthyl 4-*n*-nonanoyl-oxybiphenyl-4′-carboxylate (C9) and *s*-2-methylbuthyl 4-*n*-decanoyl-oxybiphenyl-4′-carboxylate (C10) synthesized by one of the authors. These compounds have the following phase sequence: isotropic → Sm A → Sm C* → crystalline.

The sample cell was made of patterned indium-tin oxide-coated glass substrates (0.8 cm × 0.8 cm). Both sides of the glass substrates were coated with buffed polymer layers followed by rubbing to promote homogeneous alignment. The cell thickness was maintained using glass spacers of 3 μm diameters.

Spontaneous polarization was measured by a triangular wave method,[12)] which is easy for subtracting background current. Polarization current, converted into a voltage signal through an amplifier, was measured using a digitizing oscilloscope (TDS 420, Tektronics). Dielectric constant was measured using an impedance analyzer (4192A, HP). The cell was mounted in a microfurnace (FP90, Mettler) for temperature control, and temperature fluctuations were 0.1°C.

3. Results and Discussion

Figure 1 shows that the temperature dependence of spontaneous polarization for C9 (circles) and C10 (rectangles) compounds measured with a triangular wave of 5 V/μm, which is sufficient for unwinding the helix of the Sm C* phase. The polarization vanishes at a certain temperature T_i other than the critical temperature T_c, which is the Sm A–Sm C* phase transition temperature. Due to the polarization inversion occurring at T_i, it is regarded as the polarization inversion temperature.

It is clear that the temperature dependence of spontaneous polarization is not described by the power law. To explain such polarization inversion, a model based on dynamically fluctuating molecular species was introduced.[6,11,13)] Assuming that there are only two different species in the system, spontaneous polarization, P_s, exhibits temperature dependence shown by

*E-mail address: jhkim@hallym.ac.kr

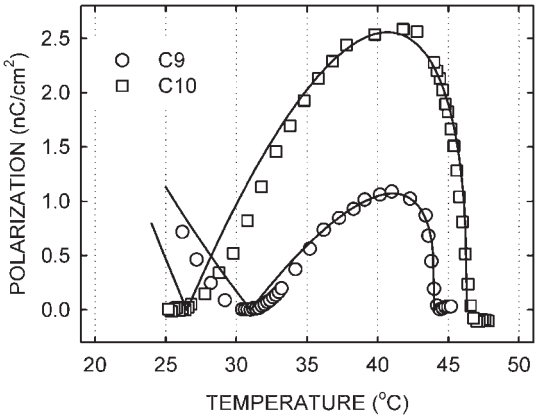

Fig. 1. Temperature dependence of the spontaneous polarization measured with a triangular wave of 5 V/μm at 30 Hz for C9 and C10 compounds. Each solid line is the least-squares fit using eq. (3.1).

Table I. The fitting parameters obtained from the fits of the data in Fig. 1 using eq. (3.1) for two compounds.

Parameters (unit)	C9	C10
P_a (C/cm^2)	-3.177×10^{-8}	-3.392×10^{-8}
P_b (C/cm^2)	8.973×10^{-8}	10.473×10^{-8}
U (eV)	0.0273	0.0291
α	0.285	0.382

$$P_s(T) = \left[\frac{P_a}{1+e^{-U/k_BT}} + \frac{P_b}{1+e^{U/k_BT}}\right](T_c - T)^{\alpha}, \qquad (3.1)$$

where U, α, and k_B are the activation energy between the two species, a critical exponent, and the Boltzmann constant, respectively. Here, P_a and P_b denote the spontaneous polarizations of each species. Because the polarization vanishes at T_i, using eq. (3.1) adopted as $P_s(T_i) = 0$, we obtained the least-squares fits, which were represented by each solid line in Fig. 1, for each compound. The experimental values of $T_c = 44°C$ and $T_i = 31°C$ for C9 and $T_c = 46.3°C$ and $T_i = 26.5°C$ for C10 were used to fit the data. The fitting parameters for C9 and C10 compounds are summarized in Table I.

Figure 2 shows the temperature dependence of dielectric constant for C9 and C10 compounds measured with various dc bias fields at 500 Hz. With increasing dc bias field, dielectric constant was reduced, owing to the suppression of the Goldstone mode under an external field. Without a dc bias field, the dielectric constant increases through the Sm A–Sm C* phase transition and reaches its maximum near $T = 40°C$ as in conventional FLCs.[14–16] With further decrease in temperature, however, the dielectric constant gradually decreases and bounces at its local minimum (corresponding to T_i). In the regime of low dc bias fields (≤ 3 V/μm), we have also observed the change in the curvature of the curves from the results of the temperature dependence of dielectric constant, which implies the anomaly of dielectric constant.

The dielectric constant in the Sm C* phase mainly originates in the Goldstone mode ϵ_G, which corresponds to the phase fluctuation around the smectic cone and is affected by the spontaneous polarization, P_s, of the system. The

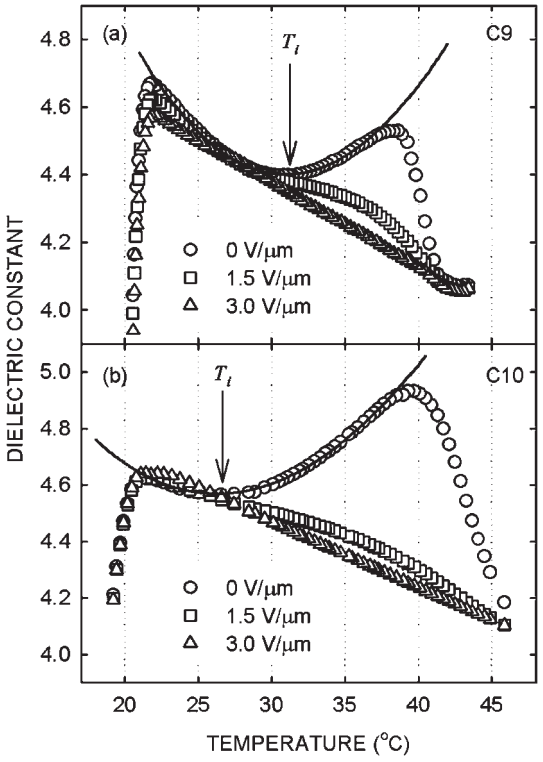

Fig. 2. Temperature dependence of the dielectric constants measured at various dc bias fields at 500 Hz for (a) C9 and (b) C10 compounds. Each solid line is the least-squares fit of the data using eq. (3.2) with no dc bias field. T_i's are the polarization inversion temperatures.

Goldstone mode is expressed as $\epsilon_G \propto (1/K_3)(P_s/q\theta)^2$, where K_3, q, and θ are the bend elastic constant, wave vector, and tilt angle, respectively.[3] Thus, ϵ_G does not depend on the sign of P_s but on the temperature dependence of P_s, θ, and helical pitch $p = 2\pi/q$. In general FLCs, however, P_s, θ, and p are almost independent of temperature far from T_c. In C9 and C10 compounds exhibiting polarization inversion, the polarization vanishes at T_i, which causes an anomalous behavior of dielectric constant. Near T_i, the spontaneous polarization is simplified as $P_s \propto (1/T - 1/T_i)$ from eq. (3.1). Using the temperature dependence of the polarization, the dielectric constant corresponding to the Goldstone mode is directly expressed as

$$\epsilon_G \propto \frac{1}{K_3}\left[\frac{P_a U}{k_B q\theta}\left(\frac{1}{T} - \frac{1}{T_i}\right)\right]^2. \qquad (3.2)$$

Each solid line in Fig. 2 is the least-squares fit of the experimental data using eq. (3.2) for each compound with no dc bias field. The polarization inversion temperatures, T_i's, were obtained by fitting the experimental data for each compound, and were as good as the experimentally determined temperatures, which were used to fit the spontaneous polarization in Fig. 1 with eq. (3.1). For C9, $T_i = 30.95°C$ and $1/K_3(q\theta)^2 = 2.542 \times 10^{-2}$ m^2/N and for C10, $T_i = 26.28°C$ and $1/K_3(q\theta)^2 = 1.437 \times 10^{-2}$ m^2/N.

Figure 3 shows dielectric constant as a function of dc bias field at various temperatures. Near the Sm A–Sm C* phase transition temperature T_c, as shown in Fig. 3(a), the dielectric constant is maximum near the zero field and is suppressed to a constant with increasing dc bias field, which is a normal behavior observed in conventional FLCs.

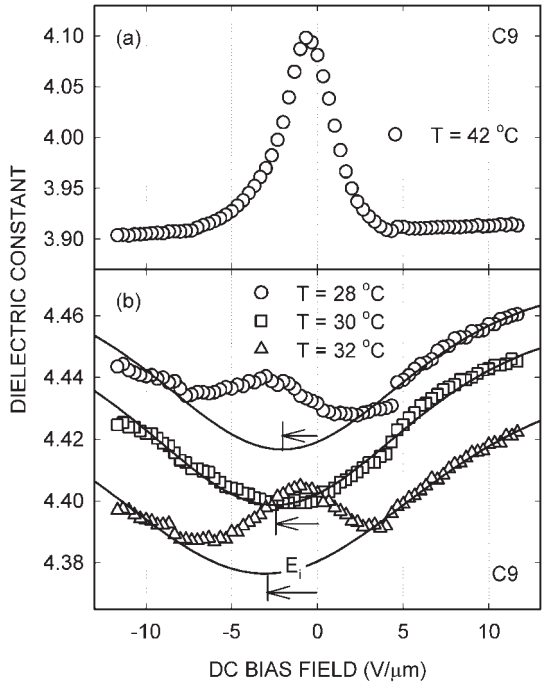

Fig. 3. Dc bias field dependence of dielectric constant at various temperatures for C9 compound: (a) normal behavior suppressed by dc bias field near T_c and (b) anomalous behavior induced by dc bias field near T_i. Each solid line in (b) is the least-squares fit for each temperature using eq. (3.4).

As temperature approaches T_i, the peak corresponding to the Goldstone mode decreases and disappears as shown in Fig. 3(b). The peak, however, reappears with further decrease in temperature below T_i. Note that the dielectric constant is not suppressed and show a non linear behavior near T_i different from that near T_c. There are two possibilities to explain these anomalous behaviors: the contribution of tilt fluctuation such as electroclinic (EC) effect and the change in the molecular density of a system with at least two different molecular species induced by an electric field. The former, however, is dominant near T_c different from the anomalous non linear behavior near T_i. Moreover, the contribution of tilt fluctuation to dielectric constant is negligible with respect to that of phase fluctuation. The latter is based on the model of dynamically fluctuating molecular species, which has already introduced to explain polarization inversion and the temperature dependence of dielectric constant. In the compounds used in this work, the applied electric field significantly alters the equilibrium densities of two conformers because of the interaction of the correlated dipole clusters with an external electric field. In the system with only two different molecular species, the density of the conformer with a dipole moment parallel to the applied electric field E is enhanced relative to that with a dipole moment antiparallel to E. Therefore, it is quite reasonable that an induced electric susceptibility should be introduced as well as the Goldstone mode.

Applying an electric field, the interaction energy ΔE between the induced effective dipole moment μ_{eff} associated with the antiparallel clusters and the applied electric field E is expressed as $\Delta E = \mu_{\text{eff}} E$.[17] Here, μ_{eff} is different from the molecular dipole moment since the effective dipole moment is generated by the clusters of molecules responding to the electric field. Such interaction energy contributes to the activation energy U introduced in eq. (3.1). Thus, the polarization including the one induced by the applied electric field is expressed as

$$P_s(T) = (T_c - T)^{\alpha} \times \left[\frac{P_a}{1 + e^{-(U+\mu_{\text{eff}}E)/k_B T}} + \frac{P_b}{1 + e^{(U+\mu_{\text{eff}}E)/k_B T}} \right]. \tag{3.3}$$

In the above system, the effective dielectric constant consists of the Goldstone mode ϵ_G corresponding to a phase fluctuation and the induced dielectric constant ϵ_I due to the relative change in the molecular densities of two conformers induced by the applied electric field. When an electric field was applied above a certain critical field, where the Goldstone mode was almost saturated to a constant value, dielectric constant was mainly affected by ϵ_I. In fact, as shown in Fig. 3(b), the peak is observed near the zero field and even disappears at T_i, which corresponds to the disappearance of the spontaneous polarization as described in eq. (3.1). Above a critical field dielectric constant slowly increases with ϵ_I. This quantity is related to the average induced polarization of the corresponding mode by $\epsilon_I(T) \propto \partial P_I / \partial E$.[3] Therefore, the induced dielectric constant ϵ_I can be expressed from eq. (3.3) as

$$\epsilon_I \propto \frac{\mu_{\text{eff}}}{k_B T} (T_c - T)^{\alpha} \times \frac{P_a - P_b}{[e^{-(U+\mu_{\text{eff}}E)/2k_B T} + e^{(U+\mu_{\text{eff}}E)/2k_B T}]^2} + \epsilon', \tag{3.4}$$

where ϵ' is a constant. At the polarization inversion temperature T_i, represented by rectangular symbols in Fig. 3(b), we fitted the result with eq. (3.4) and represented the fitting result as a solid line. For other temperatures, the peak near the zero field was cut off to exclude the Goldstone mode and each solid line was represented as the result fitted with eq. (3.4).

In Fig. 3(b), note that the minimum points of the solid lines, where the contribution to the induced dielectric constant changes from one conformer to the other, are shifted from the zero field. These shifts originate from the activation energy between two conformers. Thus, the electric field corresponding to the minimum dielectric constant implies an inversion electric field changing the contribution to the induced dielectric constant. In addition, we can confirm the inversion of the contribution to the dielectric constant because the position of the inversion electric field, E_i, relative to the electric field, E_{MAX}, with a maximum dielectric constant in a low-field regime changes at T_i. In other words, $E_{\text{MAX}} < E_i$ for $T < T_i$ (circles) and $E_{\text{MAX}} > E_i$ for $T > T_i$ (triangles), as shown in Fig. 3(b). E_i is obtained by differentiating eq. (3.4) with E. Using $\partial \epsilon_I / \partial E = 0$, the inversion electric field E_i is simply achieved as $E_i = -U/\mu_{\text{eff}}$. Note that E_i is negative since $U > 0$ and $\mu_{\text{eff}} > 0$.

Figure 4 shows the induced effective dipole moment $|\mu_{\text{eff}}|$ obtained from the least-squares fitting of the dielectric constant induced by a dc bias electric field with eq. (3.4). Since Sm A phase is a paraelectric phase, if the polarization induced by the EC effect is neglected, $|\mu_{\text{eff}}|$ has to vanish at the Sm A–Sm C* phase transition temperature T_c. The

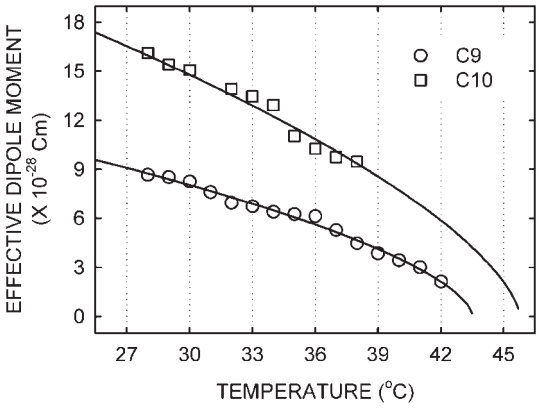

Fig. 4. Temperature dependence of the induced effective dipole moment $|\mu_{\text{eff}}|$ for each compound. Each solid line is the least-squares fit using eq. (3.5).

induced effective dipole moment obtained from Fig. 3 for each temperature was fitted using the simple power law as a function of temperature as

$$|\mu_{\text{eff}}| = \mu_0(T_c - T)^{\beta}, \tag{3.5}$$

where μ_0 and β are the proportional constant of the effective dipole moment and the critical exponent, respectively. From the fits for each compound, $\mu_0 = 1.601 \times 10^{-28}$ Cm, $T_c = 43.56°$C, and $\beta = 0.618$ for C9 and $\mu_0 = 2.487 \times 10^{-28}$ Cm, $T_c = 45.78°$C, and $\beta = 0.646$ for C10. Here, μ_0's correspond to the sum of the dipole moments of the molecular clusters responding to the applied electric field. The T_c's agree well with the experimental results for each compound.

4. Conclusions

In order to describe the anomalous dielectric behavior of FLCs exhibiting polarization sign inversion, we introduced the induced effective dipole moment into a model based on a dynamically fluctuating mixture of two interconvertible conformers whose relative densities change with external electric field. Applying an electric field, the equilibrium densities of the two conformers are significantly varied because of the interaction energy of the dipole clusters with the applied electric field. It is found that the induced effective dipole moment associated with the density variation is described by the simple power law as a function of temperature.

Acknowledgements

This work was supported in part by the Ministry of Information and Communication of Korea through IMT-2000 Project.

1) R. B. Meyer, L. Liebert, L. Strzelecki and P. Keller: J. Phys. Lett. **36** (1975) L69.
2) R. Blinc: Ferroelectrics **14** (1976) 603.
3) T. Carlsson, B. Žekš, C. Filipič and A. Levstik: Phys. Rev. A **42** (1990) 877.
4) J. W. Goodby, N. A. Clark, S. T. Lagerwall, M. A. Osipov, S. A Pikin, T. Sakurai, K. Yoshino and B. Žekš: *Ferroelectric Liquid Crystals; Principles, Properties, and Applications* (Gordon and Breach Science Publishers, Philadelphia, 1991).
5) J. W. Goodby, E. Chin, T. M. Leslie, J. M. Geary and J. S. Patel: J. Am. Chem. Soc. **108** (1986) 4729.
6) J. S. Patel and J. W. Goodby: J. Phys. Chem. **91** (1987) 5838.
7) J. W. Goodby, E. Chin, J. M. Geary, J. S. Patel and P. L. Finn: J. Chem. Soc. Faraday Trans. **83** (1987) 3429.
8) R. Eidenschink, T. Geehaar, G. Anderson, A. Dahlgren, K. Flatischier, F. Gouda, S. T. Lagerwall and K. Skarp: Ferroelectrics **84** (1988) 167.
9) H. Y. Liu, C. C. Huang, T. Min, M. D. Wand, D. M. Walba, N. A. Clark, Ch. Bahr and G. Heppke: Phys. Rev. A **40** (1989) 6759.
10) K. Yoshino, M. Ozaki, K. Nakano, H. Taniguchi, N. Yamasaki and K. Satoh: Liq. Cryst. **5** (1989) 1203.
11) J.-H. Kim, Y. Kim, S. W. Suh, S.-D. Lee and J. W. Goodby: J. Kor. Phys. Soc. **27** (1994) S185.
12) K. Miyasato, S. Abe, H. Takezoe, A. Fukuda and E. Kuze: Jpn. J. Appl. Phys. **22** (1983) L661.
13) S.-D. Lee, J. S. Patel and J. W. Goodby: Phys. Rev. Lett. **66** (1991) 449.
14) T. Sakurai, N. Mikami, M. Ozaki and K. Yoshino: J. Chem. Phys. **85** (1986) 585.
15) M. Ozaki, K. Yoshino, T. Sakurai, N. Mikami and R. Higuchi: J. Chem. Phys. **86** (1987) 3648.
16) C. Filipič, T. Carlsson, A. Levstik, B. Žekš, R. Blinc, F. Gouda, S. T. Lagerwall and K. Skarp: Phys. Rev. A **38** (1988) 5833.
17) Y. Mieda, H. Hoshi, Y. Takanishi, H. Takezoe and B. Žekš: Phys. Rev. E **67** (2003) 021701.